PERGAMON

International Journal of Solids and Structures 40 (2003) 2473–2486

INTERNATIONAL JOURNAL OF SOLIDS and STRUCTURES

www.elsevier.com/locate/ijsolstr

Stress intensity factors of a rectangular crack meeting a bimaterial interface

T.Y. Qin [a,*], N.A. Noda [b]

[a] College of Science, China Agricultural University, Box 75, Beijing 100083, PR China
[b] Department of Mechanical Engineering, Kyushu Institute of Technology, Kitakyushu 804-8550, Japan

Received 19 April 2002; received in revised form 10 December 2002

Abstract

Using the hypersingular integral equation method based on body force method, a planar crack meeting the interface in a three-dimensional dissimilar materials is analyzed. The singularity of the singular stress field around the crack front terminating at the interface is analyzed by the main-part analytical method of hypersingular integral equations. Then, the numerical method of the hypersingular integral equation for a rectangular crack subjected to normal load is proposed by the body force method, which the crack opening dislocation is approximated by the product of basic density functions and polynomials. Numerical solutions of the stress intensity factors of some examples are given.

Keywords: Stress intensity factor; Body force method; Crack; Composite material; Hypersingular integral equation

1. Introduction

In recent decades, the use of new materials is increasing in a wide range of engineering field and the accurate evaluation of interface strength in dissimilar materials becomes very important. Considerable researches have been done to evaluate the stress intensity factors and crack opening displacement for cracks in dissimilar materials (Cook and Erdogan, 1972; Lee and Keer, 1986; Chen and Nisitani, 1993). However, most of these works are on two-dimensional cases. Due to the difficult of mathematics, there are no any analytical methods for three-dimensional crack problems. However several numerical methods are available, such as the hypersingular integral equation method combined with boundary element method (Qin et al., 1997; Helsing et al., 2001). Lee and Keer (1986) evaluated the stress intensity factors of a crack meeting the interface by a body force method, but they did not give the singularity and the singular stress field near the crack front at the interface. Noda et al. (1999) studied mixed modes stress intensity factors of an inclined semi-elliptical surface crack by a body force method, in which the unknown body force densities

* Corresponding author. Tel.: +86-10-62336992; fax: +86-10-62336777.
E-mail address: mech@cau.edu.cn (T.Y. Qin).

0020-7683/02/$ - see front matter
doi:10.1016/S0020-7683(03)00015-5

were approximated by the products of fundamental density functions and polynomials. This numerical method was applied by Wang et al. (2001) to investigated the stress intensity factors of a 3D rectangular crack using body force method.

In the present paper, a hypersingular integral equation method based on the body force method is applied to solve the problem of a three-dimensional vertical crack meeting at an interface. Based on the analytical solution of singular stress field near the crack front, and the numerical approach suggested by Noda et al. (1999) will be improved to obtain highly reliable numerical results of stress intensity factors.

2. General solutions and the hypersingular integral equation for a planar crack meeting the bimaterial interface

A fixed rectangular Cartesian system x_i ($i = 1, 2, 3$) is used. Consider two dissimilar half-spaces bonded together along the x_1–x_3 plane. Suppose that the right half-space (x_2 plane) is occupied by an elastic medium with elastic constants (μ_1, ν_1) and the left half-space ($-x_2$ plane) is occupied by an elastic medium with elastic constants (μ_2, ν_2). There is a rectangular crack terminating at the bimaterial interface as shown in Fig. 1. The crack is assumed to be in a plane normal to the x_3 axis, and subjected to a normal load. Based on the body force method (Lee and Keer, 1986), the displacements in the left and right materials can be expressed as

$$u_i^m(\mathbf{x}) = \int_S T_{i3}^m(\mathbf{x}, \boldsymbol{\xi}) \tilde{u}_3(\xi)\, \mathrm{d}s(\xi) \quad i = 1, 2, 3;\ m = 1, 2 \tag{1}$$

where $\tilde{u}_3 = u_3^+ - u_3^-$ is the crack opening dislocation, the superscripts 1 and 2 denote the right and left materials respectively, and

$$T_{13}^1(\mathbf{x}, \boldsymbol{\xi}) = \frac{(x_1 - \xi_1)}{2\pi(\kappa_1 + 1)} \left\{ \frac{1 - \kappa_1}{2r_1^3} + \frac{3x_3^2}{r_1^5} - \frac{A\kappa_1(\kappa_1 - 1)}{2r_2^3} + \frac{6Ax_2\xi_2}{r_2^5} - \frac{3A(3 - \kappa_1)x_2(x_2 + \xi_2)}{r_2^5} + \frac{3A\kappa_1 x_3^2}{r_2^5} - \frac{30Ax_2\xi_2x_3^2}{r_2^5} + \frac{1}{2}(A\kappa_1^2 + 2A\kappa_1 + B - 2C)\left(\frac{1}{r_2 r_3^2} - \frac{2x_3^2}{r_2^2 r_3^3} - \frac{x_3^2}{r_2^3 r_3^2} \right) \right\} \tag{2}$$

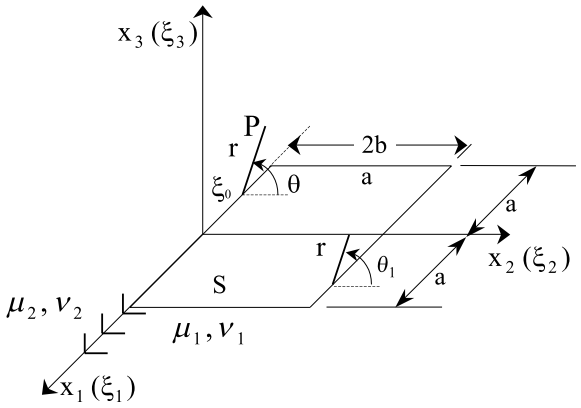

Fig. 1. Problem configuration.

$$T_{23}^{1}(\mathbf{x},\boldsymbol{\xi}) = \frac{1}{2\pi(\kappa_1+1)}\left\{(x_2-\xi_2)\left(\frac{1-\kappa_1}{2r_1^3}+\frac{3x_3^2}{r_1^5}\right)+\frac{(6A-5A\kappa_1)(x_2+\xi_2)+6A(\kappa_1-1)\xi_2}{2r_2^3}\right.$$
$$+\frac{6Ax_2\xi_2(x_2+\xi_2)}{r_2^5}-\frac{3A(3-\kappa_1)x_2(x_2+\xi_2)^2}{r_2^5}+\frac{3A\kappa_1(x_2-\xi_2)x_3^2}{r_2^5}-\frac{30Ax_2\xi_2(x_2+\xi_2)x_3^2}{r_2^5}$$
$$\left.-\frac{1}{2}(A\kappa_1^2-B)\left(\frac{1}{r_2r_3}-\frac{x_3^2}{r_2^2r_3^2}-\frac{x_3^2}{r_2^3r_3}\right)\right\} \tag{3}$$

$$T_{33}^{1}(\mathbf{x},\boldsymbol{\xi}) = \frac{x_3}{2\pi(\kappa_1+1)}\left\{\frac{\kappa_1-1}{2r_1^3}+\frac{3x_3^2}{r_1^5}+\frac{2C-A\kappa_1(3+\kappa_1)}{2r_2^3}+\frac{18Ax_2\xi_2}{r_2^5}-\frac{3A(3-\kappa_1)x_2(x_2+\xi_2)}{r_2^5}\right.$$
$$\left.+\frac{3A\kappa_1x_3^2}{r_2^5}-\frac{30Ax_2\xi_2x_3^2}{r_2^5}+\frac{1}{2}(A\kappa_1^2+2A\kappa_1+B-2C)\left(\frac{3}{r_2r_3^2}-\frac{2x_3^2}{r_2^2r_3^3}-\frac{x_3^2}{r_2^3r_3^2}\right)\right\} \tag{4}$$

$$T_{13}^{2}(\mathbf{x},\boldsymbol{\xi}) = \frac{(x_1-\xi_1)}{2\pi(\kappa_1+1)}\left\{\frac{(1-\kappa_1)(1+A\kappa_1)}{2r_1^3}+\frac{3(1+A\kappa_1)x_3^2}{r_1^5}+\frac{1}{2}(A\kappa_1^2+2A\kappa_1+B-2C)\right.$$
$$\left.\times\left(\frac{1}{r_1r_4^2}-\frac{2x_3^2}{r_1^2r_4^3}-\frac{x_3^2}{r_1^3r_4^2}\right)+\frac{1}{\Gamma}(A-B)x_2\left(\frac{1}{r_1^2r_4^2}+\frac{1}{r_1^3r_4}-\frac{2x_3^2}{r_1^3r_4^3}-\frac{3x_3^2}{r_1^4r_4^2}-\frac{3x_3^2}{r_1^5r_4}\right)\right\} \tag{5}$$

$$T_{23}^{2}(\mathbf{x},\boldsymbol{\xi}) = \frac{1}{2\pi(\kappa_1+1)}\left\{\frac{(1-\kappa_1)(1-A)(x_2-\xi_2)-2(A-B)x_2}{2\Gamma r_1^3}+\frac{3[(1-A)(x_2-\xi_2)+(A-B)x_2]x_3^2}{\Gamma r_1^5}\right.$$
$$\left.-\frac{1}{2}(A\kappa_1^2-B)\left(\frac{1}{r_1r_4}-\frac{x_3^2}{r_1^2r_4^2}-\frac{x_3^2}{r_1^3r_4}\right)\right\} \tag{6}$$

$$T_{33}^{2}(\mathbf{x},\boldsymbol{\xi}) = \frac{x_3}{2\pi(\kappa_1+1)}\left\{\frac{2C+2\kappa_1-2A\kappa_1-(1+\kappa_1)(1+A\kappa_1)}{2r_1^3}+\frac{3(1+A\kappa_1)x_3^2}{r_1^5}\right.$$
$$+\frac{1}{2}(A\kappa_1^2+2A\kappa_1+B-2C)\left(\frac{3}{r_1r_4^2}-\frac{2x_3^2}{r_1^2r_4^3}-\frac{x_3^2}{r_1^3r_4^2}\right)$$
$$\left.+\frac{1}{\Gamma}(A-B)x_2\left(\frac{3}{r_1^2r_4^2}+\frac{3}{r_1^3r_4}-\frac{2x_3^2}{r_1^3r_4^3}-\frac{3x_3^2}{r_1^4r_4^2}-\frac{3x_3^2}{r_1^5r_4}\right)\right\} \tag{7}$$

and

$$r_1=\sqrt{(x_1-\xi_1)^2+(x_2-\xi_2)^2+x_3^2},\quad r_2=\sqrt{(x_1-\xi_1)^2+(x_2+\xi_2)^2+x_3^2},\quad r_3=r_2+x_2+\xi_2,$$
$$r_4=r_2-x_2+\xi_2,\quad A=(1-\Gamma)/(1+\kappa_1\Gamma),\quad B=(\kappa_2-\kappa_1\Gamma)/(\Gamma+\kappa_2),\quad S=(1-\Gamma)/(1+\Gamma),$$
$$\Gamma=\mu_2/\mu_1,\quad C=S(\kappa_1+1),\quad \kappa=3-4\nu$$

The corresponding stress field is given as follows:

$$\sigma_{ij}^{1}(\mathbf{x})=\int_S\left\{\frac{2\mu_1\nu_1}{1-2\nu_1}\frac{\partial T_{k3}^{1}(\mathbf{x},\boldsymbol{\xi})}{\partial x_k}\delta_{ij}+\mu_1\left[\frac{\partial T_{i3}^{1}(\mathbf{x},\boldsymbol{\xi})}{\partial x_j}+\frac{\partial T_{j3}^{1}(\mathbf{x},\boldsymbol{\xi})}{\partial x_i}\right]\right\}\tilde{\boldsymbol{u}}_3(\xi)\,\mathrm{d}s(\xi)\quad j,k=1,2,3 \tag{8}$$

$$\sigma_{ij}^{2}(\mathbf{x})=\int_S\left\{\frac{2\mu_2\nu_2}{1-2\nu_2}\frac{\partial T_{k3}^{2}(\mathbf{x},\boldsymbol{\xi})}{\partial x_k}\delta_{ij}+\mu_2\left[\frac{\partial T_{i3}^{2}(\mathbf{x},\boldsymbol{\xi})}{\partial x_j}+\frac{\partial T_{j3}^{2}(\mathbf{x},\boldsymbol{\xi})}{\partial x_i}\right]\right\}\tilde{\boldsymbol{u}}_3(\xi)\,\mathrm{d}s(\xi) \tag{9}$$

Using the boundary condition, the hypersingular integral equation for unknown function $\tilde{u}_3$ can be obtained (Lee and Keer, 1986)

$$\frac{\mu_1}{\pi(\kappa_1+1)} \oint\!\!\!\!\!\!= _S \left[\frac{1}{r_1^3} + K_0(\mathbf{x},\boldsymbol{\xi})\right] \tilde{u}_3(\xi)\,\mathrm{d}s(\xi) = -p(\mathbf{x}) \tag{10}$$

where $\oint\!\!\!\!\!\!=$ is the symbol of the finite-part integral, and

$$K_0(\mathbf{x},\boldsymbol{\xi}) = \frac{2S(\kappa_1+1) - 3A(\kappa_1^2 - 2\kappa_1 + 3)}{2r_2^3} + \frac{3A[12x_2\xi_2 - (3-\kappa_1)(\kappa_1-1)(x_2+\xi_2)^2]}{2r_2^5} + \frac{3(B - 2S + 2A\kappa_1 + A\kappa_1^2 - 2S\kappa_1)}{2r_2 r_3^2} \tag{11}$$

in which $r_1 = \sqrt{(x_1-\xi_1)^2 + (x_2-\xi_2)^2}$, $r_2 = \sqrt{(x_1-\xi_1)^2 + (x_2+\xi_2)^2}$. Notice that Eq. (10) is a hypersingular integral equation, and can be numerically solved.

3. Singular stresses near the crack front meeting the interface

According to the theory of the hypersingular integral equation, the crack dislocation near a point $\boldsymbol{\xi_0}$ at the interface can be assumed as

$$\tilde{u}_3(\boldsymbol{\xi}) = D(\boldsymbol{\xi_0})\xi_2^{\lambda} \quad 0 < \mathrm{Re}(\lambda) < 1 \tag{12}$$

where $D(\boldsymbol{\xi_0})$ is a non-zero constant related to point $\boldsymbol{\xi_0}$, λ is the stress singular index near the crack front meeting the interface. Using the main-part analytical method (Tang and Qin, 1993) and following relations,

$$\oint\!\!\!\!\!\!= _{S_\varepsilon} \frac{\tilde{u}_3}{r_1^3}\,\mathrm{d}\xi_1\,\mathrm{d}\xi_2 \cong -2\pi\lambda D(\xi_0)x_2^{\lambda-1}\cot(\lambda\pi) \tag{13}$$

$$\int_{S_\varepsilon} \frac{\tilde{u}_3}{r_2^3}\,\mathrm{d}\xi_1\,\mathrm{d}\xi_2 \cong 2\pi\lambda D(\xi_0)x_2^{\lambda-1}\frac{1}{\sin(\lambda\pi)} \tag{14}$$

$$\int_{S_\varepsilon} \frac{x_2\xi_2}{r_2^5}\tilde{u}_3\,\mathrm{d}\xi_1\,\mathrm{d}\xi_2 \cong -\frac{2}{9}\pi\lambda(\lambda^2-1)D(\xi_0)x_2^{\lambda-1}\frac{1}{\sin(\lambda\pi)} \tag{15}$$

$$\int_{S_\varepsilon} \frac{(x_2+\xi_2)^2}{r_2^5}\tilde{u}_3\,\mathrm{d}\xi_1\,\mathrm{d}\xi_2 \cong \frac{4}{3}\pi\lambda D(\xi_0)x_2^{\lambda-1}\frac{1}{\sin(\lambda\pi)} \tag{16}$$

$$\int_{S_\varepsilon} \frac{\tilde{u}_3}{r_2 r_3^2}\,\mathrm{d}\xi_1\,\mathrm{d}\xi_2 \cong \frac{2}{3}\pi\lambda D(\xi_0)x_2^{\lambda-1}\frac{1}{\sin(\lambda\pi)} \tag{17}$$

where S_ε is a small area on crack surface near point $\boldsymbol{\xi_0}$, from Eq. (10), the stress singular index can be determined by

$$4A\lambda^2 + 2\cos(\lambda\pi) - A - B = 0 \tag{18}$$

This is coincident with the characteristic equation for the two-dimensional case (Cook and Erdogan, 1972; Chen and Nisitani, 1993). The stress intensity factors along the crack front meeting the interface and the inner crack front are defined as

$$K_{\mathrm{I},\lambda} = \lim_{r\to 0} \sigma_{33}(r,\theta)_{|\theta=\pi}(2r)^{1-\lambda} \tag{19}$$

$$K_{\mathrm{I}} = \lim_{r\to 0} \sigma_{33}(r,\theta'_1)_{|\theta'_1=0}\sqrt{2r} \tag{20}$$

Based on relation (12), the singular stress field around the crack front terminating at the interface can be obtained by the main-part analytical method. For a point p near the crack front point $\boldsymbol{\xi_0}$ in the right material, using following relations,

$$\int_{S_\varepsilon} \frac{\tilde{u}_3}{r_1^3}\,\mathrm{d}\xi_1\,\mathrm{d}\xi_2 \cong \frac{2\pi D(\boldsymbol{\xi_0})r^{\lambda-1}\sin(\pi-\theta)\lambda}{\sin(\lambda\pi)\sin\theta} \tag{21}$$

$$\int_{S_\varepsilon} \frac{\tilde{u}_3}{r_2^3}\,\mathrm{d}\xi_1\,\mathrm{d}\xi_2 \cong \frac{2\pi D(\boldsymbol{\xi_0})r^{\lambda-1}\sin\lambda\theta}{\sin(\lambda\pi)\sin\theta} \tag{22}$$

$$\int_{S_\varepsilon} \left[\frac{3}{r_2 r_3^2} - \frac{6x_3^2}{r_2^3 r_3^2} - \frac{12x_3^2}{r_2^2 r_3^3} + \frac{6x_3^4}{r_2^3 r_3^4} + \frac{6x_3^4}{r_2^4 r_3^3} + \frac{3x_3^4}{r_2^5 r_3^2}\right]\tilde{u}_3\,\mathrm{d}\xi_1\,\mathrm{d}\xi_2 \cong \frac{2\pi\lambda D(\boldsymbol{\xi_0})r^{\lambda-1}\cos(1-\lambda)\theta}{\sin\lambda\pi} \tag{23}$$

where $r_1 = [(x_1-\xi_1)^2 + (x_2-\xi_2)^2 + x_3^2]^{1/2}$, $r_2 = [(x_1-\xi_1)^2 + (x_2+\xi_2)^2 + x_3^2]^{1/2}$, the singular stress can be expressed by

$$\begin{aligned}\sigma_{33}^1(p) = \frac{K_{\mathrm{I},\lambda}}{\phi(2r)^{1-\lambda}}\{&-2(1-\lambda)\sin\theta\sin(\pi\lambda+2\theta-\lambda\theta) - 2\cos(\pi\lambda+\theta-\lambda\theta)\\ &+ [A(1-2\lambda)(2+\lambda)+B]\cos(1-\lambda)\theta - A(1-\lambda)(1-2\lambda)\cos(3-\lambda)\theta\}\end{aligned} \tag{24}$$

here $\phi = (2 - A - B + 2\lambda A - 2\lambda B)$. For a point p near the crack front point $\boldsymbol{\xi_0}$ in the left material, using (21) and following relations,

$$\int_{S_\varepsilon} \left[\frac{3}{r_1 r_4^2} - \frac{6x_3^2}{r_1^3 r_4^2} - \frac{12x_3^2}{r_1^2 r_4^3} + \frac{6x_3^4}{r_1^3 r_4^4} + \frac{6x_3^4}{r_1^4 r_4^3} + \frac{3x_3^4}{r_1^5 r_4^2}\right]\tilde{u}_3\,\mathrm{d}\xi_1\,\mathrm{d}\xi_2 \cong -\frac{2\pi\lambda D(\boldsymbol{\xi_0})r^{\lambda-1}\cos(\pi\lambda+\theta-\lambda\theta)}{\sin\lambda\pi} \tag{25}$$

$$\begin{aligned}&\int_{S_\varepsilon} \left[\frac{3}{r_1^3 r_4} + \frac{3}{r_1^2 r_4^2} - \frac{18x_3^2}{r_1^5 r_4} - \frac{18x_3^2}{r_1^4 r_4^2} - \frac{12x_3^2}{r_1^3 r_4^3} + \frac{15x_3^4}{r_1^7 r_4} + \frac{15x_3^4}{r_1^6 r_4^2} + \frac{12x_3^4}{r_1^5 r_4^3} + \frac{6x_3^4}{r_1^4 r_4^4}\right]\tilde{u}_3\,\mathrm{d}\xi_1\,\mathrm{d}\xi_2\\ &\quad\cong \frac{\pi\lambda(1-\lambda)D(\boldsymbol{\xi_0})r^{\lambda-1}}{\sin\lambda\pi}[\cos(\pi\lambda+\theta-\lambda\theta)+\cos(\pi\lambda+3\theta-\lambda\theta)]\end{aligned} \tag{26}$$

the singular stress can be expressed by

$$\sigma_{33}^2(p) = \frac{K_{\mathrm{I},\lambda}}{\phi(2r)^{1-\lambda}}[2(1-\lambda)(B-1)\sin\theta\cos(\pi\lambda+3\theta-\lambda\theta) - \lambda\cos(\pi\lambda+\theta-\lambda\theta)] \qquad \frac{\pi}{2}\leqslant\theta\leqslant\frac{3\pi}{2} \tag{27}$$

Other stresses near point $\boldsymbol{\xi_0}$ can be obtained by use of above method. In the case of homogeneous materials, solutions (24) and (27) are the same as that obtained by Tang and Qin (1993). The stress intensity factors along the crack front meeting the interface can be rewritten as follows:

$$K_{\mathrm{I},\lambda} = \lim_{\xi_2\to 0} \frac{\mu_1\lambda\gamma\tilde{u}_3 2^{1-\lambda}}{(\kappa_1+1)(\sin\lambda\pi)\xi_2^\lambda} \tag{28}$$

4. Numerical procedure

Using its behavior near the crack front, the crack dislocation of a rectangular crack can be written as

$$\tilde{\boldsymbol{u}}_3(\xi_1,\xi_2) = F(\xi_1,\xi_2)\xi_2^{\lambda}\sqrt{(a^2-\xi_1^2)(2b-\xi_2)} \tag{29}$$

To solve the unknown function $\tilde{\boldsymbol{u}}_3$, the unknown function $F(\xi_1,\xi_2)$ is approximately expressed

$$F(\xi_1,\xi_2) = \sum_{m=0}^{M}\sum_{n=0}^{N} a_{mn}\xi_1^m\xi_2^n \tag{30}$$

where a_{mn} is unknown constant. Substituting (29) and (30) into (10), a set of algebraic linear equations for unknown a_{mn} can be obtained

$$\sum_{m=0}^{M}\sum_{n=0}^{N} a_{mn}I_{mn}(x_1,x_2) = -\frac{\pi(\kappa_1+1)}{\mu_1}p(x_1,x_2) \tag{31}$$

where

$$I_{mn}(x_1,x_2) = I^1_{mn}(x_1,x_2) + I^2_{mn}(x_1,x_2) \tag{32}$$

in which

$$I^1_{mn}(x_1,x_2) = \oint\!\!\!\!\!\!-_S \frac{1}{r_1^3}\xi_1^m\xi_2^{\lambda+n}\sqrt{(a^2-\xi_1^2)(2b-\xi_2)}\,\mathrm{d}\xi_1\,\mathrm{d}\xi_2 \tag{33}$$

$$I^2_{mn}(x_1,x_2) = \int_S K_0(\mathbf{x},\boldsymbol{\xi})\xi_1^m\xi_2^{\lambda+n}\sqrt{(a^2-\xi_1^2)(2b-\xi_2)}\,\mathrm{d}\xi_1\,\mathrm{d}\xi_2 \tag{34}$$

The integral (34) is general ones, and can be numerically calculated. The integral (33) is hypersingular, and must be treated before being numerically evaluated. Using the Taylor's expansion and the polar coordinates $\xi_1 - x_1 = r_1\cos\theta_1$, $\xi_2 - x_2 = r_1\sin\theta_1$ as shown in Fig. 2, following relations can be obtained

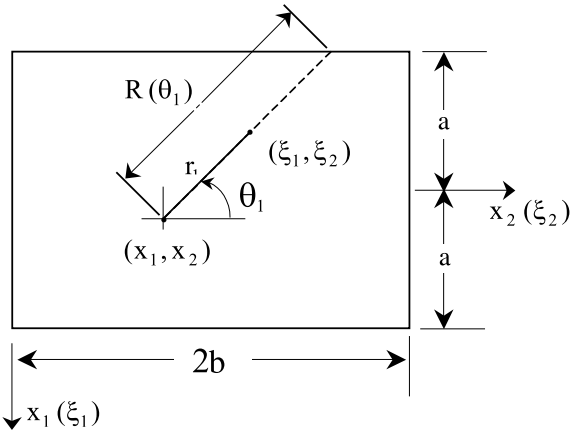

Fig. 2. Integral parameters.

$$\xi_1^m\sqrt{a^2-\xi_1^2}=\begin{cases}\sqrt{a^2-x_1^2}-\dfrac{x_1}{\sqrt{a^2-x_1^2}}r_1\cos\theta_1-Q_1(x_1,\xi_1,\theta_1)r_1^2, & m=0\\ x_1^m\sqrt{a^2-x_1^2}+\dfrac{x_1^{m-1}}{\sqrt{a^2-x_1^2}}[ma^2-(m+1)x_1^2]r_1\cos\theta_1+Q_2(x_1,\xi_1,\theta_1)r_1^2, & m>0\end{cases} \tag{35}$$

$$\xi_2^{\lambda+n}\sqrt{2b-\xi_2}=x_2^{\lambda+n}\sqrt{2b-x_2}+\frac{x_2^{\lambda+n-1}}{2\sqrt{2b-x_2}}[4b(\lambda+n)-(2\lambda+2n+1)x_2]r_1\sin\theta_1+Q_3(x_2,\xi_2,\theta_1)r_1^2 \tag{36}$$

where

$$Q_1(x_1,\xi_1,\theta_1)=\frac{a^2(x_1+\xi_1)}{\sqrt{a^2-x_1^2}\left(\sqrt{a^2-x_1^2}+\sqrt{a^2-\xi_1^2}\right)\left(\xi_1\sqrt{a^2-x_1^2}+x_1\sqrt{a^2-\xi_1^2}\right)}\cos^2\theta_1 \tag{37}$$

$$Q_2(x_1,\xi_1,\theta_1)=\begin{cases}\dfrac{1}{2(a^2-x_1^2)^{3/2}}[m(m-1)a^4x_1^{m-2}-(m^2+1)a^2x_1^m+m(m+1)x_1^{m+2}]\cos^2\theta_1, & \xi_1=x_1\\ \dfrac{1}{r_1^2}\left\{\xi_1^m\sqrt{a^2-\xi_1^2}-x_1^m\sqrt{a^2-x_1^2}-\dfrac{x_1^{m-1}}{\sqrt{a^2-x_1^2}}[ma^2-(m+1)x_1^2](\xi_1-x_1)\right\}, & \xi_1\neq x_1\end{cases} \tag{38}$$

$$Q_3=\begin{cases}\dfrac{x_2^{\lambda+n-2}}{2(a^2-x_1^2)^{3/2}}\{16(\lambda+n)(\lambda+n-1)b^2-8b(\lambda+n)(2\lambda+2n-1)x_2+[4(\lambda+n)^2-1]x_2^2\}\sin^2\theta_1, & \xi_2=x_2\\ \dfrac{1}{r_1^2}\left\{\xi_2^{\lambda+n}\sqrt{2b-\xi_2}-x_2^{\lambda+n}\sqrt{2b-x_2}-\dfrac{x_2^{\lambda+n-1}}{2\sqrt{2b-x_2}}[4b(\lambda+n)-(2\lambda+2n+1)x_2](\xi_2-x_2)\right\}, & \xi_2\neq x_2\end{cases} \tag{39}$$

Using relations (35) and (36), the kernel of integral (34) can be written as follows:

$$\xi_1^m\xi_2^{\lambda+n}\sqrt{(a^2-\xi_1^2)(2b-\xi_2)}=D_0(x_1,x_2)+D_1(x_1,x_2,\theta_1)r_1+D_2(x_1,x_2,r_1,\theta_1)r_1^2 \tag{40}$$

where $D_0(x_1,x_2)$, $D_1(x_1,x_2,\theta_1)$, and $D_2(x_1,x_2,r_1,\theta_1)$ are known functions. Using the finite-part integral method and relation (40), the hypersingular integral (33) can be reduced as

$$I_{mn}^1(x_1,x_2)=\int_0^{2\pi}\left[-\frac{D_0(x_1,x_2)}{R(\theta_1)}+D_1(x_1,x_2,\theta_1)\ln R(\theta_1)+\int_0^{R(\theta_1)}D_2(x_1,x_2,r_1,\theta_1)\,\mathrm{d}r_1\right]\mathrm{d}\theta \tag{41}$$

Now the integral in (33) is general, and can be calculated numerically. From (12), (28) and (29), the stress intensity factor at the crack front point $\boldsymbol{\xi_0}$ on the interface can be evaluated as follows:

$$K_{\mathrm{I},\lambda}=\frac{\mu_1\lambda[2-(1-2\lambda)A-(1+2\lambda)B]}{(\kappa_1+1)\sin(\lambda\pi)}2^{1-\lambda}\sqrt{2b(a^2-x_1^2)}F(x_1,0)\qquad -a\leqslant x_1\leqslant a \tag{42}$$

5. Numerical results

Consider a rectangular crack meeting the interface in three-dimensional infinite elastic solid under a uniform tension load σ_{33}^{∞} in infinity. In demonstrating the numerical results, the following dimensionless stress intensity factor of the interface crack front $F_{1,\lambda}$ and inner crack front F_1 will be used

$$F_{1,\lambda} = K_{\mathrm{I},\lambda}/\sigma_{33}^{\infty} b^{1-\lambda} \tag{43}$$

$$F_1 = K_{\mathrm{I}}/\sigma_{33}^{\infty}\sqrt{b} \tag{44}$$

5.1. Compliance of boundary condition and convergence of numerical solutions

Fig. 3 shows the compliance of the boundary condition along the crack surface for $a/b = 1$, $\mu_2/\mu_1 = 2$, $v_1 = v_2 = 0.3$, where the collocation point number is 400 (20×20). In solving the algebraic equation (31), the least square method is applied to minimize the residual stress at the collocation points. It is shown that the remaining stress $((\sigma_{33}/\sigma_{33}^{\infty}) + 1)$ on the crack surface is less than 4.5×10^{-4} when $M = N = 9$, less than 3.3×10^{-5} when $M = N = 11$, and less than 1.4×10^{-5} when $M = N = 13$.

In the case of homogeneous materials, the numerical results of dimensionless stress intensity factor with increasing the polynomial exponents are given in Tables 1 and 2 for different number of collocation points, and compared with those given by Wang et al. (2001). It is shown that the results are convergent, and the collocation point number 20×20 and the polynomial exponents $M = N = 9$ are enough for a satisfied result precision in this case. In general, too large polynomial exponents cannot give reliable results. The polynomial exponents M, N depend on the collocation point number. For the polynomial exponents $M = N = 16$, the results of the collocation point number 20×20 are not good, but the ones of the collocation point number 30×30 are satisfied. The maximum stress intensity factor is $F_{1,\lambda} = 0.7534$, and is the same as that obtained by Helsing et al. (2001) and Wang et al. (2001). In general case, Tables 3 and 4 give

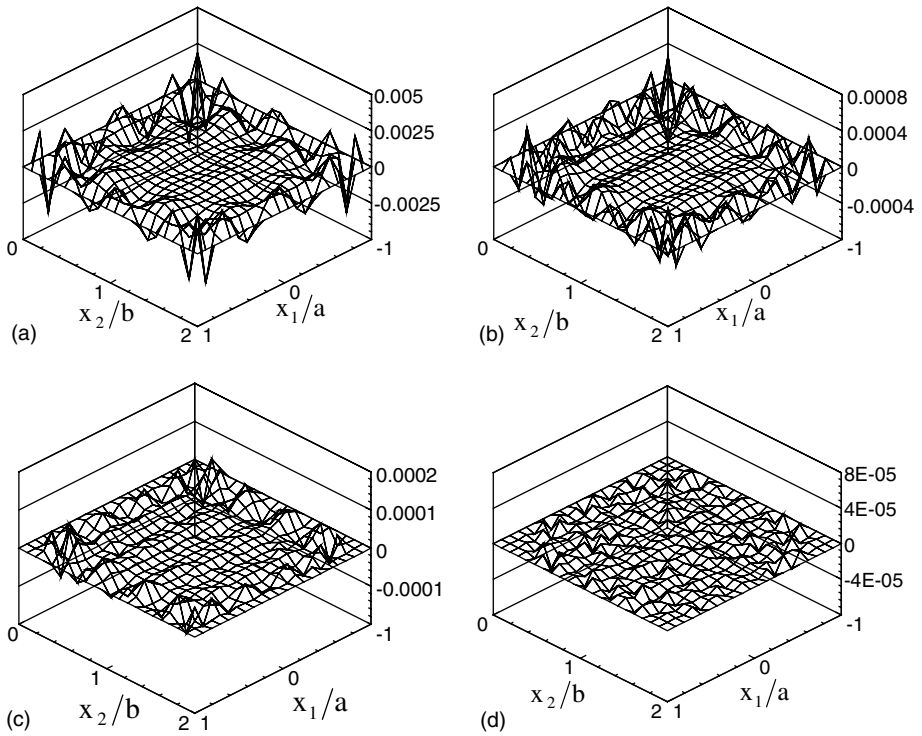

Fig. 3. Compliance of boundary condition $\sigma_{33}/\sigma_{33}^{\infty} = -1$ when $a/b = 1$, $\mu_2/\mu_1 = 2$, $v_1 = v_2 = 0.3$. (a) $M = N = 7$, (b) $M = N = 9$, (c) $M = N = 11$ and (d) $M = N = 13$.

Table 1
Convergence of dimensionless stress intensity factor $F_{1,\lambda}$ along $x_2 = 0$ with increasing the polynomial exponents $M = N$

	x_1/a										
	0/11	1/11	2/11	3/11	4/11	5/11	6/11	7/11	8/11	9/11	10/11
$M = 4$	0.7557	0.7536	0.7473	0.7370	0.7229	0.7050	0.6824	0.6530	0.6117	0.5471	0.4295
$M = 6$	0.7527	0.7512	0.7465	0.7381	0.7252	0.7069	0.6825	0.6511	0.6099	0.5504	0.4431
$M = 7$	0.7527	0.7512	0.7465	0.7381	0.7252	0.7069	0.6825	0.6511	0.6099	0.5504	0.4431
$M = 8$	0.7536	0.7518	0.7464	0.7374	0.7245	0.7067	0.6829	0.6512	0.6092	0.5504	0.4493
$M = 9$	0.7536	0.7518	0.7464	0.7374	0.7244	0.7067	0.6829	0.6512	0.6092	0.5503	0.4493
$M = 10$	0.7534	0.7517	0.7465	0.7376	0.7245	0.7065	0.6827	0.6511	0.6088	0.5499	0.4523
$M = 11$	0.7534	0.7517	0.7466	0.7376	0.7245	0.7065	0.6827	0.6511	0.6087	0.5499	0.4520
$M = 12$	0.7534	0.7518	0.7466	0.7376	0.7244	0.7065	0.6827	0.6510	0.6084	0.5493	0.4525
$M = 13$	0.7534	0.7517	0.7465	0.7375	0.7245	0.7065	0.6826	0.6510	0.6086	0.5494	0.4543
$M = 16$	0.7543	0.7530	0.7485	0.7392	0.7248	0.7056	0.6811	0.6488	0.6077	0.5530	0.5529
Wang	0.7534	0.7517	0.7465	0.7376	0.7245	0.7066	0.6828	0.6512	0.6086	0.5492	0.4536

$a/b = 1$, $\mu_2/\mu_1 = 1$, $\nu_1 = \nu_2 = 0.3$, collocation points 20×20.

Table 2
Convergence of dimensionless stress intensity factor $F_{1,\lambda}$ along $x_2 = 0$ with increasing the polynomial exponents $M = N$

	x_1/a										
	0/11	1/11	2/11	3/11	4/11	5/11	6/11	7/11	8/11	9/11	10/11
$M = 4$	0.7566	0.7543	0.7476	0.7367	0.7221	0.7038	0.6813	0.6527	0.6128	0.5502	0.4342
$M = 6$	0.7522	0.7508	0.7466	0.7385	0.7257	0.7072	0.6823	0.6502	0.6091	0.5512	0.4473
$M = 7$	0.7522	0.7508	0.7466	0.7356	0.7258	0.7072	0.6823	0.6502	0.6091	0.5512	0.4473
$M = 8$	0.7539	0.7519	0.7463	0.7371	0.7242	0.7068	0.6833	0.6513	0.6085	0.5498	0.4519
$M = 9$	0.7539	0.7519	0.7463	0.7371	0.7242	0.7068	0.6833	0.6513	0.6085	0.5498	0.4519
$M = 10$	0.7533	0.7517	0.7466	0.7377	0.7245	0.7064	0.6827	0.6514	0.6087	0.5491	0.4535
$M = 11$	0.7533	0.7517	0.7466	0.7377	0.7245	0.7064	0.6827	0.6514	0.6087	0.5491	0.4535
$M = 12$	0.7535	0.7517	0.7465	0.7376	0.7245	0.7066	0.6827	0.6512	0.6087	0.5488	0.4540
$M = 13$	0.7535	0.7517	0.7465	0.7376	0.7245	0.7066	0.6828	0.6513	0.6087	0.5488	0.4540
$M = 16$	0.7534	0.7517	0.7465	0.7376	0.7245	0.7066	0.6829	0.6514	0.6087	0.5485	0.4539

$a/b = 1$, $\mu_2/\mu_1 = 1$, $\nu_1 = \nu_2 = 0.3$, collocation points 30×30.

Table 3
Convergence of $F_{1,\lambda}$ and F_1 for $a/b = 1$, $\mu_2/\mu_1 = 0.001$, $\nu_1 = \nu_2 = 0.3$, collocation points 20×20 at $x_1 = 0$

	$F_{1,\lambda}$ $(x_2 = 0)$	F_1 $(x_2 = 2b)$
$M = N = 6$	0.001524	0.8076
$M = N = 7$	0.001524	0.8075
$M = N = 8$	0.001523	0.8085
$M = N = 9$	0.001523	0.8086

the convergence of the dimensionless stress intensity factors with increasing the polynomial exponents for $\mu_2/\mu_1 = 0.001$ and $\mu_2/\mu_1 = 10$ at points $(0, 0)$ and $(0, 2b)$.

5.2. Comparison with the two-dimensional case

If the crack is very long, e.g. a/b is very large, and tend to infinity, it is degenerated to a two-dimensional crack problem. For the case of $a/b = 8$, the polynomial exponents $M = N = 9$, and the collocation point

Table 4
Convergence of $F_{1,\lambda}$ and F_1 for $a/b = 1$, $\mu_2/\mu_1 = 10$, $\nu_1 = \nu_2 = 0.3$, collocation points 20×20 at $x_1 = 0$

	$F_{1,\lambda}$ $(x_2 = 0)$	F_1 $(x_2 = 2b)$
$M = N = 6$	2.352	0.7281
$M = N = 7$	2.345	0.7302
$M = N = 8$	2.343	0.7293
$M = N = 9$	2.342	0.7307

Table 5
Dimensionless stress intensity factors $F_{1,\lambda}$ for $a/b = 8$ and $a/b = \infty$ (Chen and Nisitani, 1993) at $x_1 = 0$, $x_2 = 0$

		β								
		−0.4	−0.3	−0.2	−0.1	0.0	0.1	0.2	0.3	0.4
$\alpha = -0.95$	$a/b = 8$	7.79	3.83	2.45	1.78	1.36				
	$a/b = \infty$	7.78	3.77	2.46	1.79	1.39				
$\alpha = -0.65$	$a/b = 8$	6.60	3.40	2.263	1.66	1.29				
	$a/b = \infty$	6.73	3.39	2.254	1.67	1.30				
$\alpha = 0.05$	$a/b = 8$			1.45	1.16	0.985	0.825	0.708		
	$a/b = \infty$			1.47	1.17	0.967	0.818	0.701		
$\alpha = 0.65$	$a/b = 8$					0.424	0.393	0.365	0.343	0.327
	$a/b = \infty$					0.434	0.400	0.373	0.351	0.331
$\alpha = 0.95$	$a/b = 8$					0.074	0.073	0.072	0.073	0.075
	$a/b = \infty$					0.077	0.075	0.074	0.076	0.078

number is 20×20. The stress intensity factors at the center of the crack front on the interface are given in Table 5, and compared with the result given by Chen and Nisitani (1993). In which, $\alpha = [\kappa_2 + 1 - \Gamma(\kappa_1 + 1)]/[\kappa_2 + 1 + \Gamma(\kappa_1 + 1)]$, $\beta = [\kappa_2 - 1 - \Gamma(\kappa_1 - 1)]/[\kappa_2 + 1 + \Gamma(\kappa_1 + 1)]$. It is shown that the error is large for $\alpha \to 1$ $(\Gamma \to 0)$, the maximum error is about 3.9%.

5.3. Comparison for a rectangular crack in an infinite materials and a rectangular surface crack in a half space

Now the polynomial exponents are also taken as $M = N = 9$, and the collocation point number is 20×20. For a rectangular crack in a homogeneous material, Table 6 gives the maximum stress intensity factor for different ratios of a/b. It is shown that present results are closed to those given by Wang et al. (2001) and Isida et al. (1991). If $\mu_2/\mu_1 \to 0$, it is the case of a surface crack in a half space. The dimensionless stress intensity factors at the crack front point ($x_1 = 0$, $x_2 = 2b$) are given in Table 7. It is shown that present results are close to the results obtained later (Isida et al., 1991; Noda and Wang, 2000).

Table 6
Dimensionless stress intensity factor $F_{1,\lambda}$ for $\mu_2/\mu_1 = 1$, $\nu_1 = \nu_2 = 0.3$ at $x_1 = 0$, $x_2 = 0$

	a/b						
	1	2	4	5	8	10	∞
Present	0.753	0.906	0.977	0.987	0.995	0.999	1.000
Wang	0.753	0.906	0.977	–	0.995	–	–
Isida	0.756	0.907	0.977	–	0.995	–	–

Table 7
Dimensionless stress intensity factor F_1 for $\mu_2/\mu_1 = 0$, $\nu_1 = 0.3$ at $x_1 = 0$, $x_2 = 2b$

	a/b					
	1	2	4	8	10	∞
Present	0.810	1.113	1.387	1.531	1.552	1.586
Noda	0.810	1.112	1.386	1.529	1.550	1.586
Isida	0.803	1.069	1.318	1.481	–	1.586

Table 8
Dimensionless stress intensity factor $F_{1,\lambda}$ for $\nu_1 = \nu_2 = 0.3$ at $x_1 = 0$, $x_2 = 0$

	μ_2/μ_1							
	0.01 ($\lambda = 0.0852$)	0.1 ($\lambda = 0.2338$)	0.5 ($\lambda = 0.4255$)	1.0 ($\lambda = 0.5000$)	2.0 ($\lambda = 0.5661$)	10.0 ($\lambda = 0.6672$)	50.0 ($\lambda = 0.7013$)	100.0 ($\lambda = 0.7061$)
$a/b = 1$	0.015	0.122	0.456	0.754	1.17	2.34	2.97	3.08
$a/b = 2$	0.023	0.171	0.572	0.904	1.36	2.58	3.24	3.34
$a/b = 8$	0.032	0.215	0.651	0.997	1.46	2.69	3.34	3.44
$a/b = \infty$	0.033	0.220	0.656	1.000	1.467	2.694	3.337	3.444

5.4. Solutions for general cases

For general cases, the polynomial exponents are taken as $M = N = 9$, and the collocation point number is 20×20 for the following results. Table 8 and Fig. 4 give the maximum dimensionless stress intensity factors at the center of the crack front on the interface varied with the ratio of μ_2/μ_1 for different ratios of a/b, Table 9 and Fig. 5 give the maximum dimensionless stress intensity factors at the center of the inner crack front parallel to the interface. It can be shown that the stress intensity factors vary more gently when $\mu_2/\mu_1 \geqslant 10$. The dimensionless stress intensity factors along the crack front meeting the interface are shown in Figs. 6 and 7 for different ratios of a/b and μ_2/μ_1, and compared with two-dimensional cases. It is shown

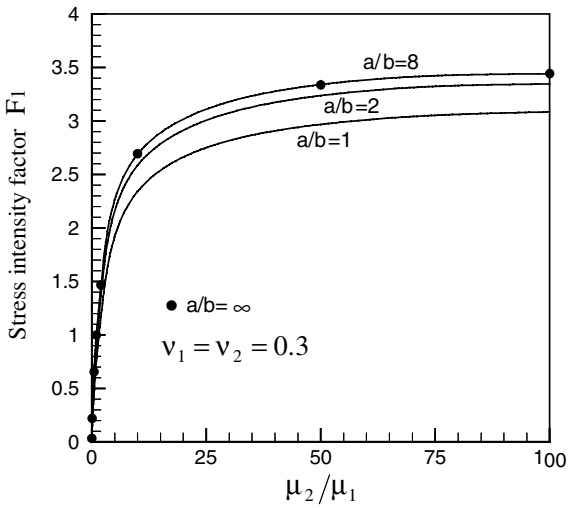

Fig. 4. Stress intensity factor $F_{1,\lambda}$ at the center of the interface crack front ($x_2 = 0$).

Table 9
Dimensionless stress intensity factor F_1 for $v_1 = v_2 = 0.3$ at $x_1 = 0$, $x_2 = 2b$

	μ_2/μ_1							
	0.0	0.1	0.5	1.0	2.0	10.0	50.0	100.0
$a/b = 1$	0.810	0.789	0.765	0.753	0.741	0.731	0.727	0.726
$a/b = 2$	1.11	1.02	0.938	0.906	0.877	0.844	0.835	0.833
$a/b = 8$	1.53	1.24	1.06	0.995	0.947	0.889	0.874	0.872
$a/b = \infty$	1.586	1.267	1.067	1.0000	0.9501	0.8911	0.8753	0.8731

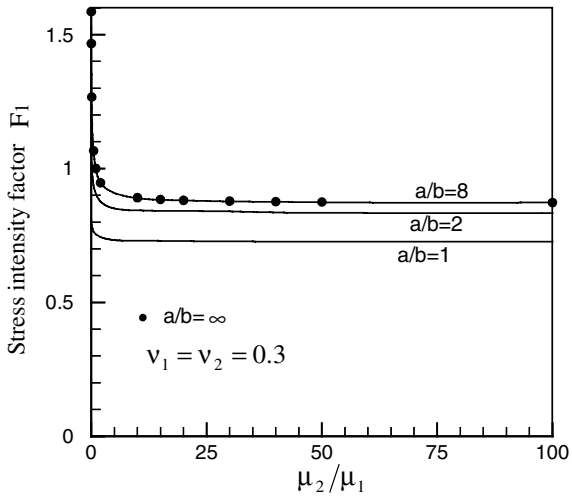

Fig. 5. Stress intensity factor F_1 at the inner crack front ($x_2 = 2b$).

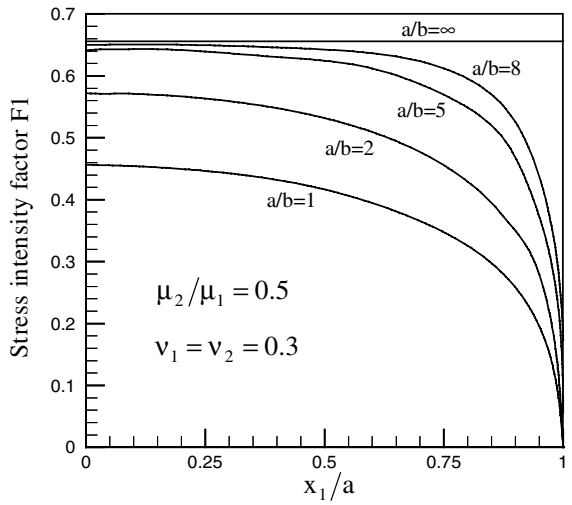

Fig. 6. Stress intensity factor $F_{1,\lambda}$ along the crack front on the interface for $\mu_2/\mu_1 = 0.5$.

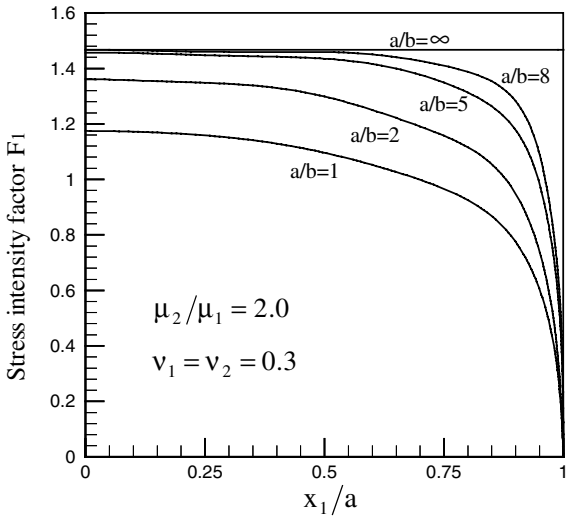

Fig. 7. Stress intensity factor $F_{1,\lambda}$ along the crack front on the interface or $\mu_2/\mu_1 = 2$.

that the stress intensity factor at the center of the crack front for the case of $a/b \geqslant 8$ is closed to that of two-dimensional case.

6. Conclusion

A rectangular crack meeting the interface in a three-dimensional dissimilar materials subjected to a normal load is studied by a hypersingular integral equation based on the body force method.

(1) The stress singularity and singular stress field around the crack front terminating at the interface are obtained by the main-part analytical method. Although expressions of the displacements and stresses in the materials are complex in modality, the solutions of singular stresses around the crack front are briefly. Due to the complexity of the stress singularities at the crack corners, it is not discussed here.
(2) The unknown function of the hypersingular integral equation is approximated by a product of a series of power polynomials and a fundamental solution, which exactly expresses the singularities of stresses near the crack front. The numerical results show that this numerical technique is successful, and the solution precision is satisfied.
(3) From the numerical solutions, it is shown that the stress intensity factors vary more gently when $\mu_2/\mu_1 \geqslant 10$, and the stress intensity factor at the center of the crack front for the case of $a/b \geqslant 8$ is closed to that of two-dimensional case.

Acknowledgements

The authors wish to thank the Inoue Foundation for Science and the 75th Commemoration Fund of Kyushu Institute of Technology for the financial supports. The useful comments and suggestions provided by the reviewers are also gratefully acknowledged.

References

Chen, D.H., Nisitani, H., 1993. Stress intensity factors of a crack meeting the bimaterial interface. Trans. Jpn. Soc. Mech. Engng. 59A, 47–53 (in Japanese).

Cook, T.S., Erdogan, F., 1972. Stresses in bonded materials with a crack perpendicular to the interface. Int. J. Solids Struct. 10, 677–697.

Helsing, J., Jonsson, A., et al., 2001. Evaluation of the mode I stress intensity factor for a square crack in 3D. Engng. Fract. Mech. 68, 605–612.

Isida, M., Yoshida, T., et al., 1991. A rectangular crack in an infinite solid, a semi-infinite solid and a finite-thickness plate subjected to tension. Int. J. Fract. 52, 79–90.

Lee, J.C., Keer, L.M., 1986. Study of a three-dimensional crack terminating at an interface. ASME J. Appl. Mech. 53, 311–316.

Noda, N.A., Wang, Q., 2000. Application of body force method to fracture and interface mechanics of composites. Research Report of the JSPS Postdoctoral Fellowship for Foreign Researchers. No. 98187.

Noda, N.A., Kobayashi, K., et al., 1999. Variation of mixed modes stress intensity factors of an inclined semi-elliptical surface crack. Int. J. Fract. 100, 207–225.

Qin, T.Y., Chen, W.J., Tang, R.J., 1997. Three-dimensional crack problem analysis using boundary element method with finite-part integrals. Int. J. Fract. 84, 191–202.

Tang, R.J., Qin, T.Y., 1993. Method of hypersingular integral equations in three-dimensional fracture mechanics. Acta Mechanica Sinica 25, 665–675.

Wang, Q., Noda, N.A., et al., 2001. Variation of the stress intensity factor along the front of a 3D rectangular crack by using a singular integral equation method. Int. J. Fract. 108, 119–131.